A Comparison of the Brightness Temperatures and Water Vapor Path Delays Measured by the TOPEX, *ERS-1,* and *ERS-2* Microwave Radiometers

JACQUES STUM

Space Oceanography Division, Collecte Localisation Satellites, Ramonville Saint-Agne, France

(Manuscript received 27 November 1996, in final form 24 September 1997)

ABSTRACT

Nadir-looking microwave radiometers are flown on altimeter missions to correct the altimeter range for water vapor path delay. This paper describes a technique to intercalibrate the brightness temperatures of the *ERS-1* and *ERS-2* microwave radiometers by using the TOPEX radiometer as a common reference. The technique is based on the analysis of radiometer measurements made at crossover points between TOPEX, *ERS-1,* and *ERS-2* orbits with less than 1-h time lags. This provides about 1000 comparison points within 4 months and covers most atmospheric and oceanic states. It is shown first that the *ERS-2* radiometer brightness temperatures need to be corrected to make them consistent with *ERS-1* and thus to ensure the homogeneity of the series of ERS altimeter data. The accuracy of the method is then estimated from the results of a 3-yr TOPEX/*ERS-1* data comparison and is shown to be about 0.2 K for the *ERS-2* 23.8-GHz channel and about 0.4 K for the 36.5-GHz channel. This 3-yr comparison also shows a -1 mm yr^{-1} drift in the (TOPEX/*ERS-1*) water vapor path delay difference, which needs to be confirmed with a longer time series. This technique could be used for the calibration of future radiometers placed in similar orbital configurations, such as the one to be flown on ENVISAT (relative to *ERS-2* and using TOPEX or JASON as a reference).

1. Introduction

Water vapor path delay (also called wet tropospheric correction) is one of the most critical terms in a satellite radar altimeter error budget (Fu et al. 1994). It ranges from 0 (dry, cold air) to 40 cm (wet, hot air). The most accurate way to measure it is to fly a microwave radiometer together with the radar altimeter, sensing the atmosphere at two or three frequencies, one of which is near the 22.235-GHz water vapor absorption line (Wilheit and Chang 1980) along the altimeter path (i.e., nadir viewing). The other frequencies may be chosen to correct for sea surface flux contribution (e.g., at 18 GHz) or to correct for cloud liquid water contribution (above 30 GHz). A three-channel configuration is expected to provide the most accurate water vapor path delay estimates (Keihm et al. 1995).

The *ERS-1* and *ERS-2* satellites carry a two-channel microwave radiometer, operating at 23.8 and 36.5 GHz. *ERS-1* was launched in July 1991. Its radiometer water vapor path estimates have been validated by comparing them with the ones derived from ground radio soundings, and they have shown good agreement (Eymard et al. 1996). *ERS-2* was launched on 20 April 1995. Although the *ERS-2* microwave radiometer is identical to the one on board *ERS-1,* its measurement accuracy needs to be assessed. Indeed, the prelaunch ground calibration of microwave radiometers often contains approximations or errors that may severely bias the radiometer estimates (Bernard et al. 1993; Ruf et al. 1994).

For the *ERS-2* assessment, it is desirable to collect water vapor path delay data that are as close as possible in space and time to the satellite measurements (separated by less than 200 km in space and 3 h in time). These time and space constraints prevent *ERS-1* and *ERS-2* water vapor path estimates from being compared directly: the satellites operate along the same ground tracks with about a 1-day interval. Routine ground radio soundings have often been used for radiometer data assessment, but very few comparison data points are available, particularly in the limited time (4 months) devoted to the *ERS-2* satellite commissioning phase. Analyzed fields of meteorological models can also be used to validate the radiometer water vapor path delay estimates (Stum 1994) but suffer from variations in the accuracy of their humidity retrievals with time. This is because of changes in the volume, accuracy, and suitability of the assimilated data or because of tuning of the model physics. For this reason, data from meteorological models may not be reliable enough to be used for a radiometer assessment at the level of accuracy required for altimeter missions (a few millimeters in path delay, less than 0.1 g cm^{-2} in integrated water vapor content). TO-

Corresponding author address: Mr. Jacques Stum, Collecte Localisation Satellites, 8-10, rue Hermes, Parc Technologique du Canal, 31526 Ramonville Saint-Agne, France.
E-mail: jacques.stum@cls.cnes.fr

PEX water vapor path delays probably offer the best comparison data available for that purpose.

- Numerous TOPEX/ERS orbit crossover points with less than 1-h lags are available (Stum 1994). This allows for a so-called point comparison—that is, comparison of how the two radiometers measure near-identical atmospheric states at the same place.
- The TOPEX microwave radiometer (TMR) was designed to derive the water vapor path delay for the TOPEX mission to within 1 cm. For that ambitious objective, the three channels (18, 21, and 37 GHz) were carefully calibrated using different sources of ground truth data, including upward-looking radiometers. The in-flight error budget (Ruf et al. 1994) shows accuracy of 1.5 K in brightness temperatures and about 1 cm in water vapor path delay.

The objectives of the present study are to validate the *ERS-2* water vapor path delay estimates in absolute terms, as well as to check that there is no discontinuity in accuracy between *ERS-1* and *ERS-2*. This last requirement is needed for a long, homogeneous ERS satellite altimeter data time series.

The calibration of the *ERS-2* microwave radiometer will be first derived using TOPEX/*ERS-1* and TOPEX/*ERS-2* crossover datasets corresponding to the first 4 months of the *ERS-2* satellite commissioning phase. A comparison of TOPEX and *ERS-1* over 3 yr will then be done to assess possible drifts between the two radiometers, as well as to estimate the accuracy of the derived *ERS-2* calibration.

2. Data processing

a. Data description

The *ERS-1* microwave radiometer data were produced by the French Processing and Archiving Facility (F-PAF), which is part of the European Space Agency off-line ground segment, and covered about 3 yr, from October 1992 to September 1995. Updating of this data (to account for the most recent *ERS-1* calibration results) is described in the appendix. For the *ERS-2* commissioning phase, *ERS-2* microwave radiometer data from 14 May to 8 September 1995 were provided by the Centre d'Étude des Environnements Terrestre et Planétaires (CETP) about 10 days after the measurements. Only data from the Kiruna station were available for *ERS-2* (on average, 9 orbits per day instead of 14).

TOPEX merged geophysical data records, cycles 2–97, were provided by the French Archiving, Validation and Interpretation of Satellite data in Oceanography (AVISO) center (AVISO/Altimetry 1996). For the period covering the *ERS-2* commissioning phase, we used TOPEX interim geophysical data records cycles 98–109, available at the AVISO center within about 10 days of the measurements. Thanks to this rapid availability of *ERS-2* and TOPEX data, we were able to do an initial comparison of TOPEX and *ERS-2* water vapor path delays as early as 3 weeks after the *ERS-2* launch. The aim of this first look was to check that no major problems occurred on the *ERS-2* instrument. The results of this first look (not shown here) were based on about 150 TOPEX/*ERS-2* crossover points with 3-h time lags. Although very preliminary, they confirmed that the *ERS-2* radiometer was functioning well.

b. Characteristics of the crossover datasets

TOPEX/*ERS-1* and TOPEX/*ERS-2* crossover points with less than 1-h time lags were calculated from the data described above. Over 10 000 such points were found in our 3-yr TOPEX/*ERS-1* dataset and about 1000 in the 4-month TOPEX/*ERS-2* dataset. As shown in Fig. 1 for the TOPEX/*ERS-2* dataset, these crossover points sample all geographic areas over the ocean, although half of them lie at latitudes greater than 50° because of the increasing number of TOPEX and ERS orbit intersections at these latitudes. Due to the shift in the TOPEX equator crossing local time (2 h every 10-day cycle), the maximum number of 1-h time lag TOPEX/ERS crossovers is found every 12 TOPEX cycles (i.e., every 4 months), when TOPEX descending passes have a local equator crossing time close to the sun-synchronous ERS 1030 descending local equator crossing time. The number and geographic locations of crossovers then repeat every 4 months. Consequently, the statistical sampling of the atmosphere and ocean surface by 4-month crossover datasets remains about the same.

c. Crossover editing

We eliminated points for which the (TOPEX − *ERS-1*) water vapor path delay difference varied from the mean difference by more than 2.5 cm. This eliminated about 8% of the original crossover dataset. Indeed, it is desirable to keep only data that are representative of the same atmospheric and surface conditions. This proved to be a useful criterion for removing points contaminated by sea ice or rain events (producing systematically higher path delay values for *ERS-1* than for TOPEX), as well as for removing points with large scatter induced by the atmosphere changing rapidly—that is, within 1 h, or different radiometer beamfilling [see Stum (1994) for a comparison of TOPEX and *ERS-1* radiometer fields of view].

3. Water vapor path delay and brightness temperature comparisons

a. Water vapor path delays

Figure 2 shows the water vapor path delay scatterplots of TOPEX versus *ERS-1* (top) and TOPEX versus *ERS-2* (bottom), both obtained from crossovers between TOPEX cycles 98–109, and concurrent *ERS-1* and *ERS-2*

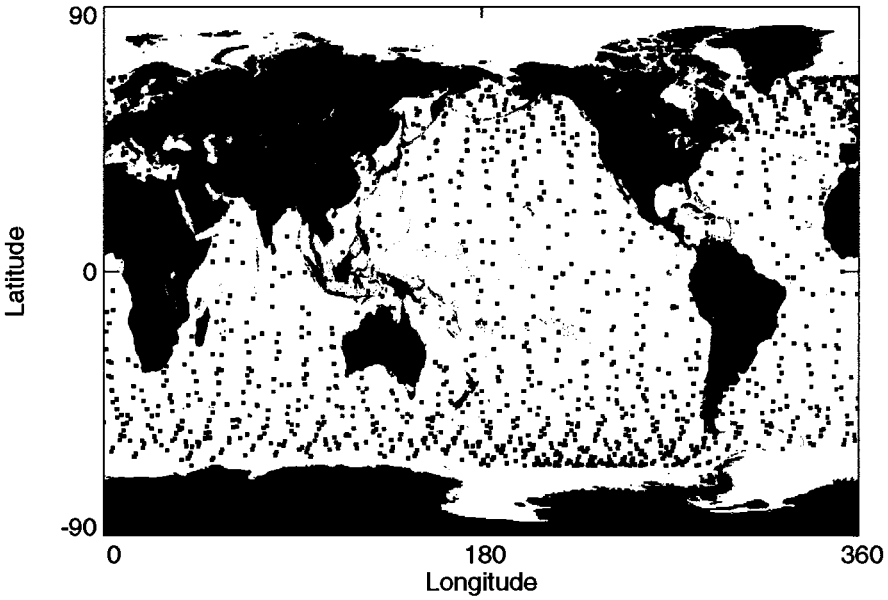

FIG. 1. Geographic location of TOPEX/*ERS-2* crossover points (13 May–8 September 1995).

data (14 May–8 September 1995). The difference between TOPEX and *ERS-1* increases from 0 (for very low path delay values) to about 1.8 cm for *ERS-1* path delays greater than 12 cm. This result is rather good, keeping in mind that the radiometers have different performances and characteristics and that the water vapor path delay retrieval schemes are also different.

It is difficult to attribute the (TOPEX − *ERS-1*) mean 1-cm difference either to a TMR overestimation or to an *ERS-1* underestimation. The difference (*ERS-1* minus radiosoundings) over a 2-yr period is zero with a standard deviation of 3 cm (Eymard et al. 1996). The difference (TOPEX minus clear-sky radiosoundings), during 1825 satellite overpasses of island launch sites from September 1992 to August 1996, is 0.23 cm with a standard deviation of 2.87 cm (C. S. Ruf 1997, personal communication). It is noteworthy, however, that comparisons carried out at the Harvest platform (B. Haynes 1997, personal communication) show an average 0.9-cm difference between TMR and an upward-looking radiometer for clear-sky overflights (0.4 cm for all weather data) and an average 1.2-cm difference between TMR and the path delay retrieved from the global positioning system (GPS) data.

There is clearly a different slope in the TOPEX/*ERS-2* relationship for *ERS-2* path delays greater than 10 cm, leading to *ERS-1*/*ERS-2* path delay differences of about 2 cm for high path delay values (more than 30 cm). This different slope cannot be attributed to the fact that the *ERS-1* crossover points are different from *ERS-2* because we can reasonably assume that the two datasets produce similar statistical sampling of the atmosphere and ocean surface. Thus, the *ERS-1*/*ERS-2* difference must be due to different brightness temperature calibration.

b. Brightness temperatures

Although the TOPEX radiometer is three-channel, operating at different frequencies (18, 21, and 37 GHz) from ERS (23.8 and 36.5 GHz), it is useful to derive a TOPEX 21-GHz versus ERS 23.8-GHz water vapor channel relationship, as well as a TOPEX 37-GHz versus ERS 36.5-GHz liquid water channel relationship. The two TOPEX/*ERS-1* channel relationships can be compared with the two TOPEX/*ERS-2* ones to investigate possible calibration deviations between *ERS-1* and *ERS-2*.

While it was desirable to include cloudy data when comparing the overall performance of the TOPEX and ERS path delay algorithms, clear skies are better for isolating and identifying calibration problems with individual radiometer channels. The TOPEX cloud liquid water content L was computed from the brightness temperatures using the algorithm given by Keihm et al. (1995). Points with $L > 0.1$ mm (equivalent to 0.1 kg m^{-2}) were eliminated. This procedure removed about 43% of points from the crossover datasets. Although the remaining points are not totally clear sky, this threshold value is probably low enough to remove the influence of heavy and medium clouds filling the TOPEX and ERS radiometer fields of view differently.

Figure 3 shows the TOPEX 21-GHz brightness temperature plotted versus the *ERS-1* (top) and *ERS-2* (bottom) 23.8-GHz brightness temperature. The brightness temperatures at 23.8 GHz, higher than at 21 GHz, are due to the shape of the 22.235-GHz water vapor absorption line, which leads to greater water vapor absorption at 23.8 GHz than at 21 GHz. The relationships between TOPEX and ERS are linear throughout the range of brightness temperatures with only slight de-

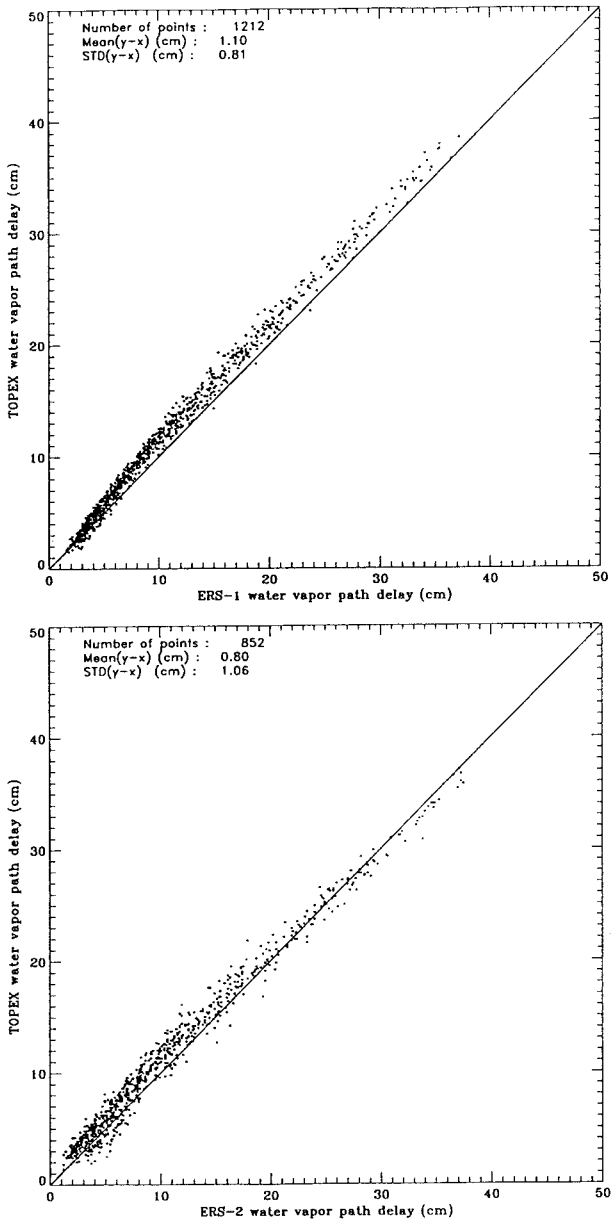

FIG. 2. Scatterplots of TOPEX vs *ERS-1* (top) and TOPEX vs *ERS-2* (bottom) water vapor path delay. Units are in centimeters. The number of points, the mean (TOPEX − ERS) difference, and the standard deviation are reported in the top left part of each plot.

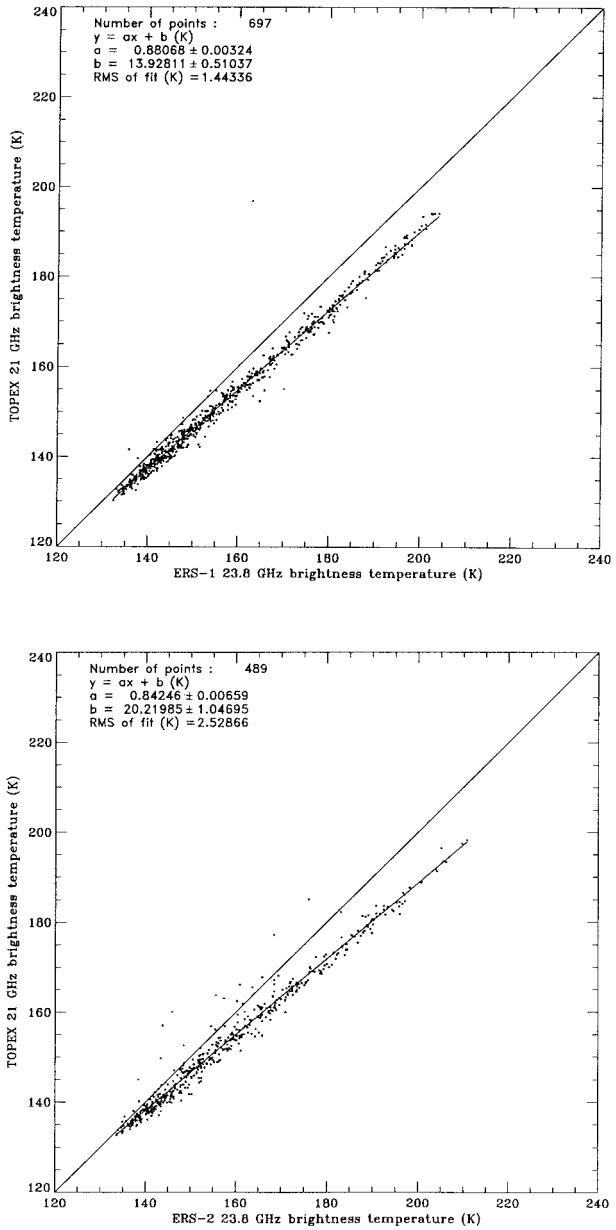

FIG. 3. Scatterplots of TOPEX 21-GHz vs ERS 23.8-GHz brightness temperatures (*ERS-1* on top, *ERS-2* on bottom). Units are in kelvins. The characteristics of the regression line are given on the top left of each plot. The standard deviation of the (TOPEX − ERS) differences about this regression line is also reported.

partures at very high values. The characteristics of these two regression lines are reported on the top left part of the plot. The increased scatter of *ERS-2* brightness temperatures relative to TOPEX, compared to *ERS-1,* is due entirely to the use of a nonoptimal *ERS-2* ground processing software during the *ERS-2* commissioning phase. The *ERS-1* and *ERS-2* slopes are different, leading to an increase with brightness temperature of the difference between *ERS-1* and *ERS-2.*

Figure 4 shows the TOPEX 37-GHz brightness temperature versus the *ERS-1* (top) and *ERS-2* (bottom) 36.5-GHz brightness temperature. Due to the elimination of cloudy points, there are no values above 180 K (keeping cloudy points would produce values up to 220 K, but the heavy clouds that fill the TOPEX and ERS fields of view differently would increase scatter and thus introduce uncertainty in the regression lines). From the comparison of the regression lines, it is clear that *ERS-1* and *ERS-2* 36.5-GHz brightness temperatures differ by more than 3 K. From the results shown in Figs. 3 and 4, it can be deduced that the *ERS-1*/*ERS-2* 23.8-

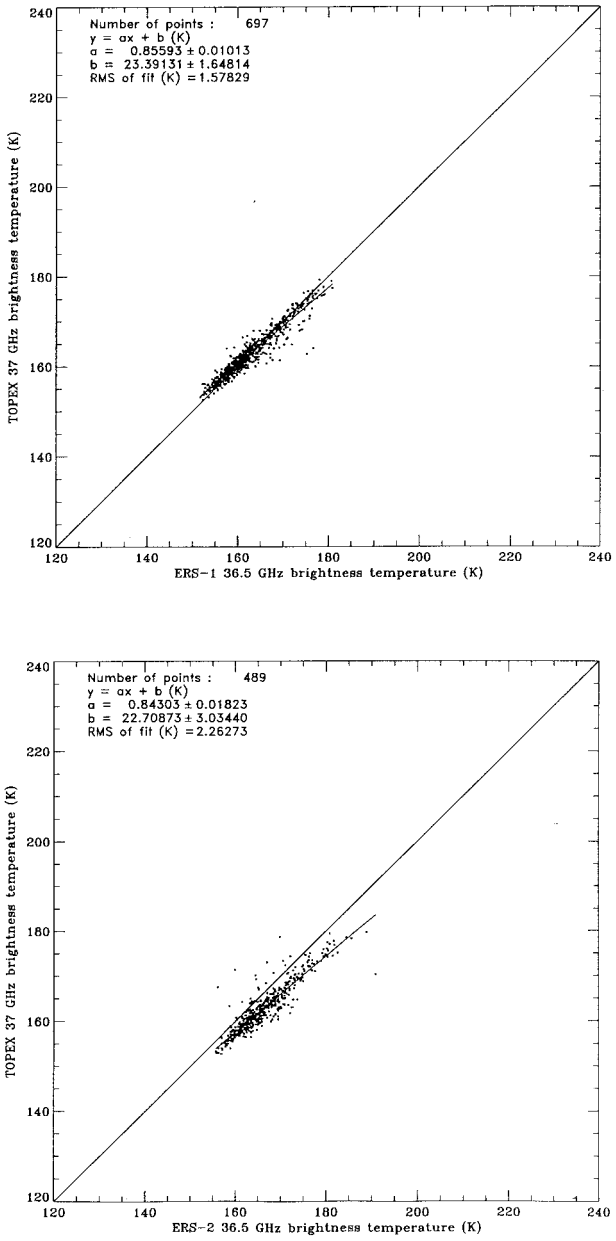

FIG. 4. Same as Fig. 3 but for TOPEX 37-GHz vs ERS 36.5-GHz brightness temperature.

GHz channel calibration difference produces the difference in slope between the *ERS-1* and *ERS-2* water vapor path delays. Indeed, the water vapor path delay is mainly sensitive to the 23.8-GHz channel brightness temperature [see Eq. (A7) in the appendix]. The increase in the difference between *ERS-1* and *ERS-2* with brightness temperature will translate into an increasing water vapor path delay difference up to 2 cm for high values. Correcting for the 36.5-GHz channel, brightness temperature error will change the path delay by only a few millimeters.

c. *ERS-2 brightness temperature corrections*

Section 3b established linear relationships between TOPEX (T) and *ERS-1* ($E1$) and between TOPEX and *ERS-2*($E2$) brightness temperatures:

$$T = a_1 E1 + b_1 \quad \text{and} \tag{1}$$

$$T = a_2 E2 + b_2, \tag{2}$$

where

$a_1 = 0.88068$, $b_1 = 13.93$, $a_2 = 0.84246$, and $b_2 = 20.22$ for the water vapor channel; and

$a_1 = 0.85593$, $b_1 = 23.39$, $a_2 = 0.84303$, and $b_2 = 22.71$ for the liquid water channel.

By combining (1) and (2), it is straightforward to derive (3) for $E1$ and $E2$:

$$E1 = AE2 + B, \tag{3}$$

where

$$A = (a_2/a_1) \quad \text{and} \tag{4}$$

$$B = (b_2 - b_1)/a_1. \tag{5}$$

If *ERS-1* data are considered to be true, then to correct *ERS-2* data, (3) has to be applied:

$$E2 \text{ corrected} = A\,E2 + B, \tag{6}$$

which yields the following two correction formulas for the *ERS-2* brightness temperatures:

$$\text{TB23.8}(ERS\text{-}2) \text{ corrected} = 0.95660 \times \text{TB23.8}(ERS\text{-}2) + 7.1 \tag{7}$$

$$\text{TB36.5}(ERS\text{-}2) \text{ corrected} = 0.98493 \times \text{TB36.5}(ERS\text{-}2) - 0.8. \tag{8}$$

As an internal consistency check, we used (7) and (8) to correct for the *ERS-2* brightness temperatures of the TOPEX/*ERS-2* crossover dataset. The water vapor path delay then has to be computed from these corrected brightness temperatures using the retrieval algorithm given by (A7) in the appendix. The TOPEX water vapor path delay is plotted in Fig. 5 versus the *ERS-2* water vapor path delay computed from corrected brightness temperatures. The behaviors of *ERS-1* and *ERS-2* relative to TOPEX are now very similar. In particular, the slope differences have been corrected, and the overall standard deviation of the (TOPEX − *ERS-2*) difference is slightly reduced (from 1.06 to 0.89 cm).

d. *Estimate of method accuracy from the TOPEX/ERS-1 3-yr crossover dataset*

The accuracy of the *ERS-2* corrections given by (7) and (8) depends on the accuracy of the a_1 and b_1 coefficients for *ERS-1* and *ERS-2* given by (1) and (2).

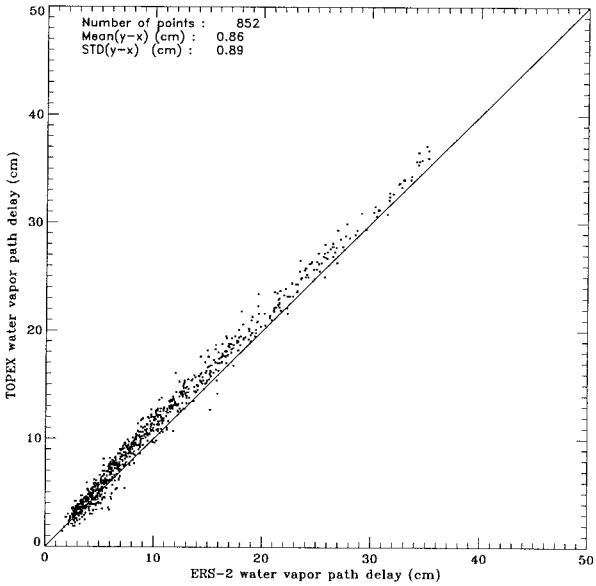

FIG. 5. Same as the bottom plot of Fig. 2 except the *ERS-2* water vapor path delay is computed from corrected brightness temperatures given by (1) and (2) (see text).

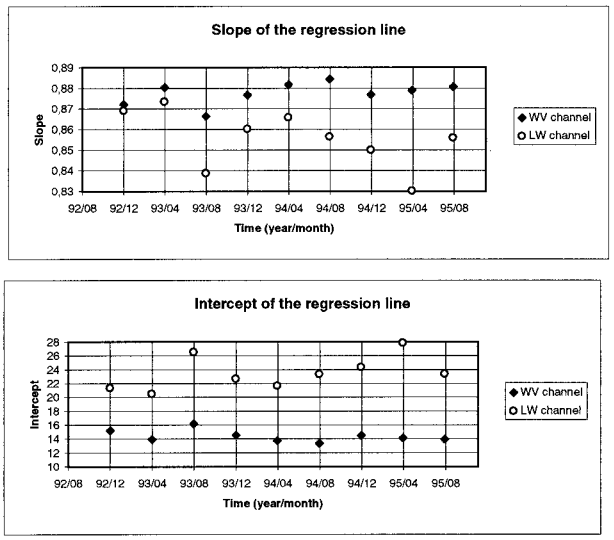

FIG. 6. Slope (top) and intercept (bottom) of the TOPEX vs *ERS-1* regression lines for the water vapor channel (diamonds) and the liquid water channel (circles), as a function of time.

This accuracy can be measured by repeating the experiment with the other 4-month time samples of the TOPEX/*ERS-1* 3-yr crossover dataset and assessing the variability of a_1 and b_2. The regression coefficients are plotted in Fig. 6 for each of the nine 4-month time samples. There is little scattering of the coefficients for the water vapor channel (21 GHz for TOPEX and 23.8 GHz for *ERS-1*), demonstrating that the sampling of atmospheric and sea surface states performed by 4-month datasets is homogeneous and that the TOPEX and *ERS-1* water vapor channels are stable over the 3-yr data record. It also confirms that the differences observed between *ERS-1* and *ERS-2* are due to real calibration differences. As expected, there is slightly more scattering on the liquid water channel because of the higher sensitivity of the brightness temperatures to variations in the radiometer beam filling, which may not have been completely removed by cloud filtering. For the liquid water channel, there seems to be a small decrease in a_1 and increase in b_1 over time.

To translate the a_1 and b_1 variations into brightness temperature variations, TOPEX brightness temperatures were computed from (1) using the regression coefficients shown in Fig. 6 and synthetic *ERS-1* brightness temperature values (130, 140, . . . , 210 K for the 23.8-GHz channel; 150, 160, . . . , 210 K for the 36.5-GHz channel). For each *ERS-1* brightness temperature value, the standard deviation of the nine TOPEX brightness temperatures was computed and is plotted in Fig. 7 as a function of *ERS-1* brightness temperature. The mean standard deviation of computed TOPEX brightness temperatures is about 0.15 K for the water vapor channel and about 0.3 K for the liquid water channel. The standard deviation is actually dependent on the *ERS-1* brightness temperature in (1) because of the small change over time of slope a_1 and intercept b_1 in Fig. 6. The minima of the curves in Fig. 7 correspond to the *ERS-1* brightness temperature value around which the regression lines rotate over time. Assuming that one should obtain the same features from equivalent 4-month time samples of TOPEX/*ERS-2* crossovers and that there is no correlation for a same 4-month dataset between the TOPEX/*ERS-1* and the TOPEX/*ERS-2* regression lines, then the estimated error on the corrected *ERS-2* brightness temperatures deduced from (6) is simply the standard deviation shown in Fig. 7 times the square root of 2.

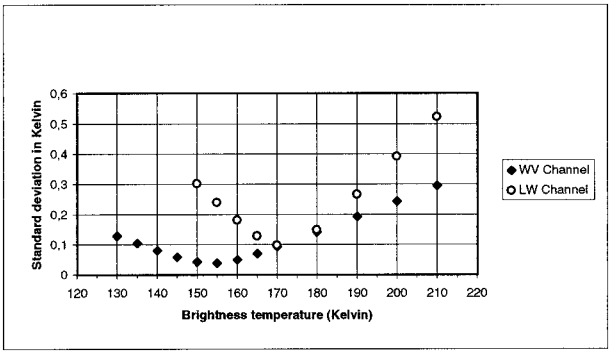

FIG. 7. Standard deviation of the nine TOPEX brightness temperatures computed from (1) using the nine sets of a_1 and b_1 coefficients shown in Fig. 6 , and synthetic *ERS-1* brightness temperature values, as a function of these synthetic *ERS-1* brightness temperature values, for the water vapor (WV) channel and for the liquid water (LW) channel.

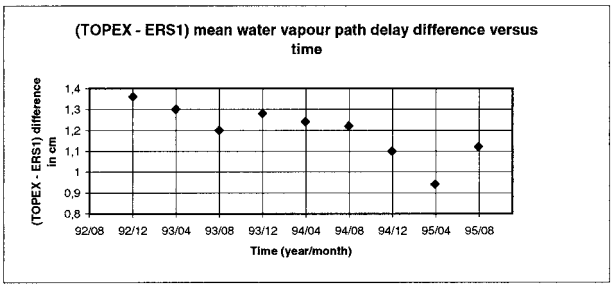

FIG. 8. (TOPEX − *ERS-1*) water vapor path delay difference as a function of time. Each point is a sample average of about 1000 crossovers.

e. TOPEX/ERS-1 water vapor path delay long-term monitoring

For each of the 4-month datasets, a mean (TOPEX − *ERS-1*) water vapor path delay difference has been computed and is plotted in Fig. 8 as function of time. The TOPEX − *ERS-1* difference appears to decrease at a rate of about −1 mm yr^{-1}. A comparison (V. Zlotnicki 1997, personal communication) between the TMR and the Defense Meteorological Satellite Program Special Sensor Microwave/Imager for 1992–96 shows a similar decrease in the (TMR − SSM/I) difference of −1.3 mm yr^{-1} in water vapor path delay. A comparison over the same period between TMR and an upward-looking radiometer (WVR) at the Harvest platform (B. Haynes 1997, personal communication) also shows a decrease in the (TMR − WVR) difference of −1.8 mm yr^{-1} in the water vapor path delay but seems to contradict the comparison with the water vapor path delay retrieved from GPS data at the same place, indicating a positive +0.2 mm yr^{-1} difference. Finally, a comparison with clear-sky radiosoundings during 1825 satellite overpasses of island launch sites (C. S. Ruf 1997, personal communication) indicates a −1.13 mm yr^{-1} drift in TMR water vapor path delay over the period September 1992–August 1996. Even though all these results are consistent and seem to indicate that the TMR water vapor path delay could drift over time, further analysis and accumulation of more data are needed before drawing such a conclusion, which could directly impact sea level rise studies carried out from the TOPEX and *ERS-1* altimeters.

4. Conclusions

An assessment of *ERS-1* and *ERS-2* two-channel radiometers was performed using the TOPEX three-channel microwave radiometer. This assessment showed general agreement at the 1–2-cm level in water vapor path delay between *ERS-1* and *ERS-2*, and TOPEX. As far as *ERS-1* and *ERS-2* are concerned, the agreement is good for water vapor path delay values smaller than 12 cm. Above this value, the estimates differ by up to 2 cm above 30 cm. Two linear equations have been derived to correct for the *ERS-2* 23.8- and 36.5-GHz channel brightness temperatures and make *ERS-1* and *ERS-2* homogeneous. It has been shown that, although derived from a limited 4-month dataset, the *ERS-2* correction was accurate to the 0.2-K level for the 23.8-GHz channel and to the 0.4-K level for the 36.5-GHz channel. The accuracy of the *ERS-2* calibration obtained with this technique makes it attractive for calibrating future radiometers placed in similar orbital configurations, such as the one to be flown on ENVISAT (relative to *ERS-2* and using TOPEX or JASON as a reference). More generally, computing crossovers between ENVISAT and JASON will be helpful for comparing their 23.8-GHz channels and water vapor path delays. Such dual crossovers can now be used for long-term monitoring of the TOPEX and *ERS-2* missions to detect possible small drifts between the radiometers. From the 3-yr TOPEX/*ERS-1* crossover dataset, there appears to be a −1 mm yr^{-1} decrease in the (TOPEX − *ERS-1*) water vapor path delay difference. This result is consistent with other unpublished comparisons of TOPEX microwave radiometer with satellite or ground truth data. This points to possible drift of the TOPEX microwave radiometer water vapor path delay over time but needs to be confirmed by further studies.

Acknowledgments. This study would not have been possible without Joel Dorandeu and Philippe Sicard, who wrote special computer codes to extract and process the TOPEX, *ERS-1*, and *ERS-2* data. The author would also like to thank everyone at CERSAT, the French Processing and Archiving Facility, for their special efforts to make all *ERS-1* Microwave Brightness Temperatures (MBT) data available. Sid-Ahmed Boukabara and Laurence Eymard from CETP kindly provided all the *ERS-2* data, as well as results from the most recently updated *ERS-1* calibration and retrieval algorithm. Most of this work has been sponsored by ESA (Purchase Order 143187 from 15/09/1994) and benefited from comments within the *ERS-2* Radar Altimeter and Microwave Radiometer Commissioning Working Group chaired by Jerome Benveniste at ESA/ESRIN. The author would like to thank Philippe Gaspar and Pierre-Yves Le Traon for their helpful suggestions and remarks.

APPENDIX

Updating *ERS-1* Data

From the *ERS-1* launch to March 1995, microwave radiometer data were distributed to users in the MBT products (CERSAT 1994), which contain the two brightness temperatures together with time, location, and land/sea flag. An initial version of the radiometer prelaunch calibration coefficients was used to produce these MBT products for the whole *ERS-1* lifetime. In September 1993, Eymard et al. (1996) improved the initial cali-

bration and derived the following equations to correct for the brightness temperatures:

$$\text{TB23.8 (1993)} = 0.96053 \times \text{TB23.8(MBT)} + 12.235 \quad \text{(A1)}$$

and

$$\text{TB36.5 (1993)} = 0.96154 \times \text{TB36.5(MBT)} + 11.81, \quad \text{(A2)}$$

where TB denotes the brightness temperature in kelvins. These correction formulas were sent to the MBT users (CLS 1993).

In June 1995 the *ERS-1* radiometer prelaunch calibration was reviewed, producing the following equations:

$$\text{TB23.8 (1995)} = \text{TB23.8 (1993)} - 2.41 \quad \text{(A3)}$$

and

$$\text{TB36.5 (1995)} = 0.98 \times \text{TB36.5 (1993)} + 1.93. \quad \text{(A4)}$$

Finally, in March 1996, a slight correction to the June 1995 calibration was added:

$$\text{TB23.8 (1996)} = 1.0037 \times \text{TB23.8 (1995)} + 0.5931 \quad \text{(A5)}$$

$$\text{TB36.5 (1996)} = 1.0108 \times \text{TB36.5 (1995)} - 2.4484. \quad \text{(A6)}$$

The water vapor path delay was calculated according to the most recently updated version of the retrieval algorithm:

$$\begin{aligned}\text{WVPD} = {} & A + B \times \ln[280 - \text{TB23.8 (1995)}] \\ & + C \times \ln[280 - \text{TB36.5 (1995)}] \\ & + D \times (U - 7)\end{aligned} \quad \text{(A7)}$$

with

$$A = 165.4353, \quad B = -54.6681,$$
$$C = +22.5584, \quad \text{and} \quad D = -0.1366.$$

This algorithm is based on the MPM'93 water vapor absorption model given by Liebe et al. (1993). In (A7), WVPD denotes the water vapor path delay in centimeters, and U denotes the sea surface windspeed in meters per second. The small correction term by sea surface wind speed is computed at TOPEX/ERS crossover points using the wind from the TOPEX altimeter.

We used and corrected (as described above) all MBT products available at the time of this study, that is, from October 1992 to March 1995, as well as the preliminary version of ocean products from April to September 1995, which contains the brightness temperatures.

REFERENCES

AVISO/Altimetry, 1996: AVISO user handbook for merged TOPEX/Poseidon products. AVI-NT-02-101-CN, Ed. 3.0, 196 pp. [Available from CLS, 8–10 rue Hermes, Parc Technologique du Canal, 31526 Ramonville St-Agne, France.]

Bernard, R., A. Le Cornec, L. Eymard, and L. Tabary, 1993: The microwave radiometer aboard *ERS-1*. Part 1: Characteristics and Performances. *IEEE Trans. Geosci. Remote Sens.,* **31,** 1186–1198.

CERSAT, 1994: Microwave radiometer products user manual. C1-EX-MUT-A21-02-CN, Issue 2, Revision 0, 05/09/94, 32 pp. [Available from CERSAT, IFREMER, BP 70, 29280 Plouzané, France.]

CLS, 1993: Quality assessment of CERSAT microwave radiometer products, 22/12/1993. CLS.OC/NT/93008, Ed. 1, 2 pp. [Available from CERSAT, IFREMER, BP 70, 29280 Plouzané, France.]

Eymard, L., L. Tabary, and A. Le Cornec, 1996: The microwave radiometer aboard *ERS-1*. Part 2: Validation of the retrieved geophysical data. *IEEE Trans. Geosci. Remote Sens.,* **34,** 291–303.

Fu, L. L, E. J. Christensen, C. A. Yamarone Jr., M. Lefebvre, Y. Ménard, M. Dorrer, and P. Escudier, 1994: TOPEX/Poseidon mission overview. *J. Geophys. Res*, **99,** 24 369–24 381.

Keihm, S. J., M. A. Janssen, and C. S. Ruf, 1995: TOPEX/Poseidon Microwave Radiometer (TMR). Part 3: Wet troposphere range correction algorithm and pre-launch error budget. *IEEE Trans. Geosci. Remote. Sens.*, **33,** 147–161.

Liebe, H. J., G. A. Hufford, and M. G. Cotton, 1993: Propagation modeling of moist air and suspended water/ice particles at frequencies below 1000 GHz. Proc. *AGARD 52d Special Meeting of the Panel on Electromagnetic Wave Propagation*, Palma de Mallorca, Spain, Advisory Group Aerosp. Res. Dev., 1–10.

Ruf, C., S. Keihm, M. Janssen, M. Subramanya, and T. Liu, 1994: TOPEX microwave radiometer performance and in-flight calibration. *J. Geophys. Res*, **99,** 24 915–24 926.

Stum, J., 1994: A comparison between TOPEX microwave radiometer, *ERS-1* microwave radiometer, and European Centre for Medium-Range Weather Forecasts derived wet tropospheric corrections. *J. Geophys. Res*, **99,** 24 927–24 939.

Wilheit, T. T., and A. T. C. Chang, 1980: An algorithm for retrieval of ocean surface and atmospheric parameters from observations of the scanning multichannel microwave radiometer. *Radio Sci.,* **15,** 525–544.